Generation of strong electric fields in an ice film capacitor

Sunghwan Shin, Youngsoon Kim, Eui-seong Moon, Du Hyeong Lee, Hani Kang et al.

Citation: J. Chem. Phys. **139**, 074201 (2013); doi: 10.1063/1.4818535
View online: http://dx.doi.org/10.1063/1.4818535
View Table of Contents: http://jcp.aip.org/resource/1/JCPSA6/v139/i7
Published by the AIP Publishing LLC.

Generation of strong electric fields in an ice film capacitor

Sunghwan Shin, Youngsoon Kim, Eui-seong Moon, Du Hyeong Lee, Hani Kang, and Heon Kang[a)]
Department of Chemistry, Seoul National University, 1 Gwanak-ro, Seoul 151-747, South Korea

(Received 14 May 2013; accepted 1 August 2013; published online 15 August 2013)

We present a capacitor-type device that can generate strong electrostatic field in condensed phase. The device comprises an ice film grown on a cold metal substrate in vacuum, and the film is charged by trapping Cs^+ ions on the ice surface with thermodynamic surface energy. Electric field within the charged film was monitored through measuring the film voltage using a Kelvin work function probe and the vibrational Stark effect of acetonitrile using IR spectroscopy. These measurements show that the electric field can be increased to $\sim 4 \times 10^8$ V m^{-1}, higher than that achievable by conventional metal plate capacitors. In addition, the present device may provide several advantages in studying the effects of electric field on molecules in condensed phase, such as the ability to control the sample composition and structure at molecular scale and the spectroscopic monitoring of the sample under electric field. © *2013 AIP Publishing LLC*. [http://dx.doi.org/10.1063/1.4818535]

I. INTRODUCTION

Electric fields play an important role in chemical reactions and influence various physical and chemical phenomena in nature. For example, the initial trajectories of reaction that bring molecules from far separation to contact distance are influenced by the electric fields that are generated from local charge, dipole moment, and polarizability of the reactants, and also by the fields from the surrounding solvents in condensed phase. Electric field has special significance in interfacial chemistry. It is believed that strong electric field exists in the electrical double layer (EDL) region of electrode/electrolyte interface and controls the nature and speed of the electrochemical reaction.[1,2] Electrophoresis, various membrane technologies, and the stability of colloidal particles are based on the existence of EDLs at the interfaces and their electrostatic interactions.[3]

Various experimental methods have been devised to generate strong electric fields and use them for investigating their effects on molecular systems. Charged parallel metal plates offer one of the simplest approaches to generate a strong electric field with the field strength of up to $\sim 10^7$ V m^{-1} inside a vacuum, or somewhat higher value in certain dielectric media.[4] This method has been widely used to observe electric field effects such as Stark effects and electrochromism of molecules.[4–9] An electric field of more than $\sim 10^7$ V m^{-1} is available within the EDL region of a routine electrochemical cell. However, the EDL thickness is very low, typically only a few nanometers or less from the electrode surface at electrolyte concentrations higher than 1 mM,[1,2] which makes it difficult to accurately measure the internal field strength of EDL by the available experimental methods.[9] Field ionization method employing a sharp metal tip can generate an extraordinarily high ($\sim 10^{10}$ V m^{-1}) field at the tip apex; this method has been used to ionize the adsorbed atoms and molecules at the tip apex.[10] Focused laser beams can generate very intense field in a time-varying (AC) mode of optical frequency.[11] For application of this method in studying the molecular systems, it is necessary to resolve the diverse physical phenomena that may arise during the interactions of laser fields with molecules.

Apparently, developing a new experimental method is crucial for the progress of research in this field. The following characteristics are desirable for the advanced experimental tool: (i) generation of electric field stronger than that achieved by conventional methods using charged metal plates ($\sim 10^7$ V m^{-1}), preferably in a DC mode; (ii) ability to control and characterize the generated field; and (iii) compatibility for studying the molecular systems, which includes sample preparation under well-controlled environment and spectroscopic monitoring of the sample under the field. In this paper, we present a new capacitor-type device that could be suitable for such purposes. This device comprises an ice film grown on a cold metal substrate in ultrahigh vacuum (UHV), where the ice film is charged by the deposition of low-energy Cs^+ ions on the surface. This work is not the first that investigates the deposition of low-energy ions onto molecular films.[12–17] Cowin and co-workers[13–15] deposited various ions onto frozen molecular films and studied the transport properties of ions through these films by using a Kelvin work-function probe. Cooks and co-workers[12,16] deposited organic molecular cations onto self-assembled monolayer surfaces and examined their trapping and release behavior. Recently, Horowitz and Asscher[17] reported that the interactions of low energy Ar^+ ions and electrons with condensed water films developed into a capacitor-like charging behavior. Also, the trapping efficiency of low-energy electrons at frozen water surfaces was studied by several research groups.[18,19] The present work is distinguished from these previous works by focusing on the generation of electric fields inside the samples. In addition, the ice film charging is driven by thermodynamic interfacial energy, which enables strong electric fields

a)Author to whom correspondence should be addressed. Electronic mail: surfion@snu.ac.kr. Tel.: +82 2 8757471.

to be developed in the film by trapping Cs^+ ions at the surface and preventing their migration to the interior.[20–22]

II. CONSTRUCTION OF ICE FILM CAPACITOR

We grew an ice film on a Ru(0001) crystal surface by H_2O vapor deposition inside a UHV chamber. The UHV chamber[12,23] had instrumentations for ion-beam deposition and *in situ* spectroscopic analysis of a sample, viz., a low-energy Cs^+-ion gun (Kimball Physics), a quadrupole mass spectrometer (QMS; Extrel), a Fourier transform infrared (FTIR) spectrometer (Perkin Elmer, Spectrum 100), and a Kelvin work function probe (McAllister). The Ru(0001) substrate surface was atomically cleaned by standard sputtering and annealing procedures. The ice film was grown to a desired thickness of 60–120 monolayers (MLs) by using a back-filling method at slow ($\leq$0.12 ML s^{-1}) deposition rate. Here, the water coverage (whether crystalline or amorphous) is given relative to the molecular density of ice Ih(0001) surface (1 ML = 1.1 × 10^{19} water molecules m^{-2}).[24] The ice film thickness was estimated by performing temperature-programmed desorption (TPD) measurements.[25] Ru substrate temperature was controlled below 120 K during the ice film growth, which resulted in amorphous ice.[24] The thickness of the ice film grown under these conditions is relatively uniform with some local variations due to the random deposition of the incident molecules on cold substrate.[22] Crystalline ice film was not used in the present experiments, because it cannot be grown to a uniform thickness because of the occurrence of roughening transition on Ru(0001), unless the thickness of the film is greater than a certain critical value.[24,26,27]

Acetonitrile (CH_3CN; AN) was used as a probe of internal electric field in vibrational Stark effect (VSE) measurement. AN molecules were trapped inside the ice sample by the following procedure: (i) amorphous H_2O film (58 ML) was grown on Ru(0001) at 120 K; (ii) AN was adsorbed to a thickness of ~60 ML onto the H_2O film surface at ~120 K; and finally (iii) amorphous H_2O film (58 ML thick) was overlaid onto the AN layer at ~70 K to form an "AN-sandwich film" (see Fig. 1). High temperature (~120 K) was used at stage (ii) to prepare the AN layer in a densely packed structure, which sharpened the band width of C≡N stretch mode, and therefore was advantageous for VSE measurement, compared to an AN layer prepared at low temperature. The use of low temperature (~70 K) at stage (iii) ensured that AN molecules did not diffuse into the upper H_2O layer. Each stage of the sample-preparation procedure was checked by analyzing the sample with reactive ion scattering (RIS), low-energy sputtering (LES),[28] and reflection absorption infrared spectroscopy (RAIRS) measurements.[22] RIS and LES analyses confirmed that all AN molecules were trapped underneath the H_2O overlayer after the completion of the sandwich structure, rather than being exposed at the sample surface.

After the construction of AN-sandwiched H_2O film, we charged it by spraying low-energy Cs^+ ions onto the sample surface. Cs^+ ions landing onto the ice film continued to stay on the surface instead of penetrating its interior. This is because of the thermodynamic affinity of Cs^+ for ice surface, which makes Cs^+ float on the ice surface regardless of its diffusivity in the film.[13,20,22] Cs^+ ions accumulating on the film surface draw the same amount of the opposite charge (electrons) at the film/metal interface, thereby generating a voltage across the film.[13] This situation can be treated as a charged parallel-plate capacitor. If the sample composition is homogeneous, the film voltage will be given by the equation $V = Q/C = \sigma d/\varepsilon_r\varepsilon_0$, where Q is surface charge of Cs^+ ions, C is the capacitance of the film, σ is the surface charge density, d is the film thickness, ε_r is the relative permittivity (dielectric constant) of the sample, and ε_0 is the vacuum permittivity. The electric field strength within the sample will be $E = \sigma/\varepsilon_r\varepsilon_0$. The film voltage and field equations for an AN-sandwich sample will be given in Sec. III A. The experiment employed Cs^+-beam current in the range (0.5–3) × 10^{-9} A, as measured by a picoammeter connected to the Ru substrate. The Cs^+ beam was used in a defocused mode to give uniform ion exposure over the entire sample surface.

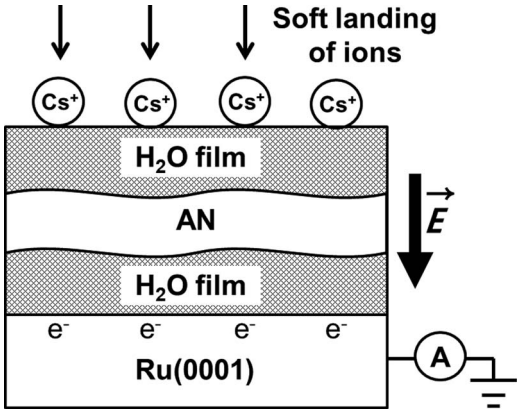

FIG. 1. Schematic of ice film capacitor. Ice film grown on a Ru(0001) metal surface is charged by depositing Cs^+ ions onto the ice surface. The sample comprises H_2O and AN layers, where AN layer is introduced as a spectroscopic probe of electric field. Ion current is read by a current meter (A) connected to the Ru substrate. More detailed description is provided in the text.

III. ELECTRIC FIELD MEASUREMENT

A. Film voltage measurement with a Kelvin probe

We characterized the electric field inside the charged ice film by two independent methods. One was the measurement of film voltage using a Kelvin work function probe,[13–15] and the other was the measurement of the vibrational Stark shift of AN molecules in the sample.[5–7] This section describes the Kelvin probe measurement.

Kelvin probe measures the contact potential difference (CPD) between the sample and the Kelvin probe, i.e., CPD = $\Phi_{probe} - \Phi_{sample}$, where Φ_{probe} and Φ_{sample} are the work functions for the gold-coated surface of probe and the sample, respectively. We are mainly interested in the film voltage developed by Cs^+ deposition, i.e., the difference of film voltages (ΔCPD) measured before and after ion deposition. Figure 2 shows ΔCPD values measured upon the exposure of sample to Cs^+ ions. The sample was an AN-sandwiched H_2O film. Cs^+-beam energy was fixed at 20 eV during the exposure. It was observed that the film voltage first increased quite linearly with the ion-exposure time; however, the increase gradually

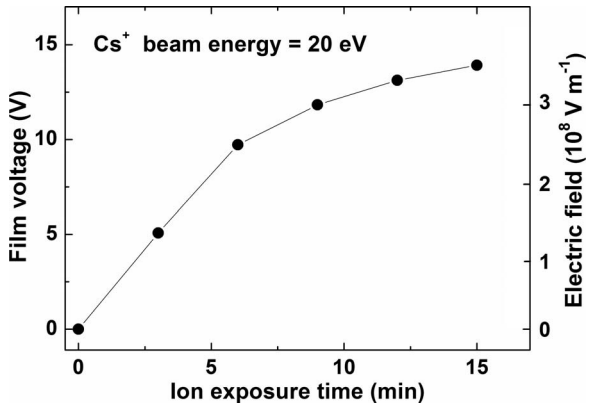

FIG. 2. Kelvin probe measurement of film voltage (ΔCPD) as a function of Cs^+-beam exposure time. The left ordinate indicates the measured film voltage, and the right ordinate indicates the electric field strength. The sample was an AN-sandwiched H_2O-ice film, which comprised H_2O(18.7 nm)/AN(20.5 nm)/H_2O(24.0 nm)/Ru(0001). The sample temperature was maintained at ~70 K during ion exposure and voltage measurement.

slowed down, and eventually the voltage reached a plateau after prolonged exposure. This saturation voltage was observed at 14 V. The Cs^+ current reading at the sample gradually decreased with increasing ΔCPD (not shown). Decrease in the ion current as well as slower increase of ΔCPD indicates that the developed film voltage reduces the sticking efficiency of incident Cs^+ ions to the film surface. This behavior is well expected, because the incoming ion trajectories will bend near the charged film where an inhomogeneous field region is developed. Although we measured the "sample current" through a picoammeter connected to the Ru substrate, it represented not only the ions arriving on the sample surface but also those reaching the other parts of the sample holder. Because it was difficult to measure only the ions reaching the sample surface, we did not know the exact amount of charges accumulated on the film.

Dividing ΔCPD with film thickness (d) gives the electric field strength (E) within the film, $E = \Delta CPD/d$. This calculation is straightforward for a sample with a homogenous matrix composition such as pure H_2O-ice film. The film thickness was estimated by measuring the water coverage in TPD experiments and from the water monolayer coverage (1.1×10^{19} molecules m^{-2} ML^{-1}) and the density of amorphous ice, assuming that the amorphous ice structure was isotropic. The dependence of the density of amorphous ice on the deposition temperature was also taken into account in the calculation.[29]

To compare the fields measured by Kelvin probe and VSE method, a sample with a sandwich structure (H_2O/AN/H_2O) was prepared. The internal field of this sample was calculated from the measured film voltage as follows. The fields in different dielectric layers differ by their relative permittivity (ε_r) factor, $E(AN):E(H_2O) = 1/\varepsilon_r(AN):1/\varepsilon_r(H_2O)$, where $E(AN)$ and $E(H_2O)$ indicate the fields inside the AN and water layers, respectively. The measured film voltage is the sum of the voltages across the AN and H_2O layers, i.e., $\Delta CPD = V(H_2O)_{top} + V(AN) + V(H_2O)_{bottom} = V(H_2O)_{total} + V(AN) = (\sigma/\varepsilon_0) \times [d(H_2O)/\varepsilon_r(H_2O) + d(AN)/\varepsilon_r(AN)]$, where $V(H_2O)_{top}$ and $V(H_2O)_{bottom}$ are the voltages across the top and bottom H_2O layers, respectively, and $V(H_2O)_{total}$ is their sum; $d(H_2O)$ is the total thickness of two H_2O layers. Using Eq. (1), it can be shown that the field strength inside the AN layer is related to the film voltage:

$$E(AN) = \Delta CPD/[d(AN) + d(H_2O)\varepsilon_r(H_2O)/\varepsilon_r(AN)]. \quad (1)$$

To calculate $E(AN)$, we need to know $d(H_2O)$, $d(AN)$, and the ε_r ratio $\varepsilon_r(H_2O)/\varepsilon_r(AN)$. We estimated $d(H_2O) = 4.27 \times 10^{-8}$ m from TPD experiments and H_2O density as 0.792 g cm^{-3}, which is the average density of amorphous ice grown at 70 K (top layer) and 120 K (bottom layer). The thickness ratio of the top and bottom H_2O layers was 1:1.29. Similarly, $d(AN) = 1.12 \times 10^{-8}$ m was estimated from the TPD experiments, which gave the relative amounts of H_2O and AN in the sample, and from the density of crystalline AN, 1.13 g cm^{-3}.[30] The $\varepsilon_r(AN)$ value of the solidified AN is unknown. Therefore, we assumed that the $\varepsilon_r(H_2O)/\varepsilon_r(AN)$ ratio in solid state at low temperature is approximately equal to the ratio of high-frequency relative permittivity (ε_∞) of liquids, which corresponds to the electronic polarizability component of ε_r. This gives $\varepsilon_\infty(H_2O)/\varepsilon_\infty(AN) = 4.57/2.26 = 2.02$.[31,32] Dipolar relaxation can only have insignificant contribution to ε_r at low temperature (~70 K) at which the present electric-field measurements were made, according to the temperature dependency of ε_r for vapor-deposited ice films reported in the literature.[13] We calculated the field strength assuming that the film has uniform thickness; however, in reality, the microscopic thickness of the samples varied due to random deposition of molecules, which could produce local field variations (Eq. (1)). However, this effect does not create problems, because both Kelvin probe and VSE methods measure the average field and the local field variations are canceled out in comparing the two results. Following the procedures mentioned above, we estimate that after 15 min of Cs^+ exposure (Fig. 2), the electric field strength inside the AN layer is 3.5×10^8 V m^{-1} and that inside the H_2O layer is 1.7×10^8 V m^{-1}. The uncertainty in this field estimation comes mostly from uncertain sample parameters, particularly from ε_r and the thickness of H_2O and AN layers. On the other hand, the accuracy of the measured film voltage is relatively good (±0.1 V). We guess that the overall uncertainty of the estimated field is <20%.

Figure 3 plots the maximum voltage across the ice film developed after the saturation of Cs^+ exposure at different beam energies (10–100 eV). The data point for 10 eV was measured after exposing the sample to Cs^+ ions at constant beam energy of 10 eV from the beginning till the point of ion saturation is reached. Then, the beam energy was raised to 20 eV. Ion exposure was continued on the same sample to the point of saturation, which gave the maximum film voltage at the beam energy of 20 eV. Similar procedures were repeated to obtain the data at the beam energies of 50 and 100 eV. Figure 3 shows that the highest film voltage obtained for this sample was 17.6 V, which was obtained at the beam energy of 50 eV. Further increasing the beam energy to beyond 50 eV was ineffective in increasing the film voltage. Experiments with samples of different thicknesses showed approximately linear proportionality between the sample thickness and the maximum film voltage (not shown). These observations indicated that the maximum field strength or maximum surface

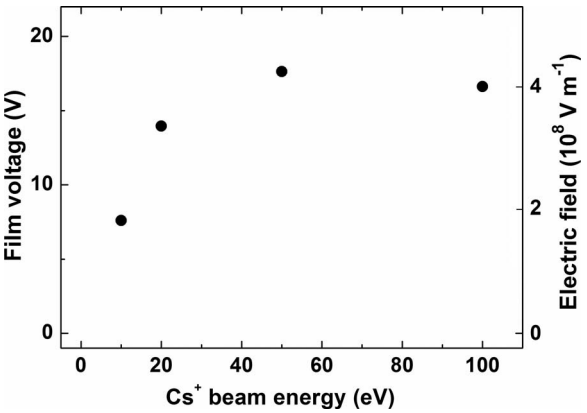

FIG. 3. Maximum film voltages attained after ion-exposure saturation at different beam energies. The estimated field strength inside the AN layer is shown along the right axis. The sample structure was H_2O(20.1 nm)/AN(19.0 nm)/H_2O(25.8 nm)/Ru(0001).

charge density was approximately the same for all samples. This, in turn, suggests the possibility that the charge-density saturation on the ice surface limits the highest field attainable in the sample. At a film voltage of 17.6 V, the estimated internal field is 4.2×10^8 V m^{-1} in the AN layer and 2.1×10^8 V m^{-1} in the H_2O layer.

The maximum charge density on the ice film surface can be limited either by the instrumental factors or by the intrinsic nature of the sample. The surface density of Cs^+ ions can be estimated from the measured film voltage. If we use $d = 6.5 \times 10^{-8}$ m and $\varepsilon_r \approx 2$ as an average value for the samples shown in Fig. 3,[13,14] the surface charge density will be $\sigma = V\varepsilon_r\varepsilon_0/d \approx 5 \times 10^{-3}$ C m^{-2} at film voltage 17.6 V. This value corresponds to the Cs^+ surface coverage of $\sim 3 \times 10^{16}$ ions m^{-2}, which is an enormously dense population of ions floating on the ice surface. If interionic Coulomb repulsion is so strong, it may be able to overcome the thermodynamic forces that hold Cs^+ ions on the surface. If this happens, the further arriving Cs^+ ions will no longer accumulate on the surface to increase the film voltage, but will rather migrate to the interior of the ice.

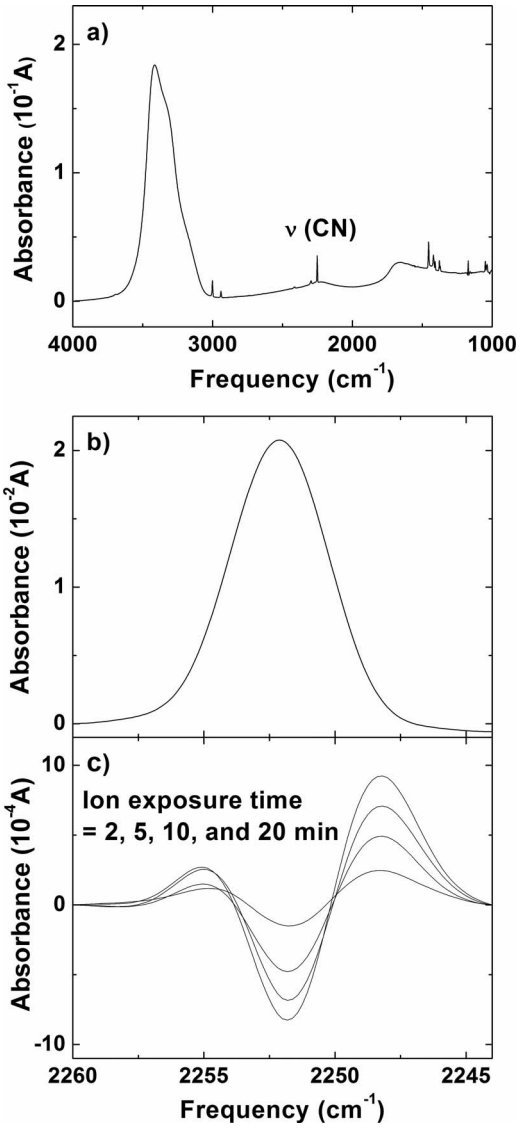

FIG. 4. (a) RAIR spectrum of an AN-sandwiched H_2O film. (b) The absorption of υ(C≡N) stretch mode (2252 cm^{-1}) shown on a magnified scale. (c) The Stark difference spectra, which show that υ(C≡N) peak became broader when the length of Cs^+ exposure, or the applied electric field, was increased. The four lines in the order of increasing shoulder intensity correspond to the ion exposures for 2, 5, 10, and 20 min, respectively. The ion beam energy was 20 eV. The sample temperature was maintained at ~70 K during ion exposure and spectral acquisition.

B. Vibrational Stark effect

We monitored the electric field inside the sample by observing VSE for the C≡N stretch frequency of AN in RAIRS experiments. Nitrile compounds have widely been used as a VSE probe,[2,5–7] because the C≡N stretch mode shows an intense and narrow band and is localized to the nitrile bond, which are the properties contributing to a strong Stark effect. The RAIRS experiments were performed with a grazing reflection angle of 84°, spectral resolution of 4 cm^{-1}, and unpolarized light from a commercial FTIR spectrometer (Perkin Elmer Spectrum 100). The VSE method measures the electric field strength at the position of the chromophore, which is called the "local electric field (**F**)."[33] The local field can be somewhat different from the externally applied field (**E**), and the difference is expressed by $\mathbf{F} = f\mathbf{E}$, where f is the local field correction factor. Exact value of f is not known, but it is generally believed to be close to unity for frozen molecular solids.[33]

A RAIR spectrum obtained from the AN-sandwiched H_2O film is shown in Fig. 4(a). The survey spectrum shows broad absorption bands characteristic of the amorphous H_2O-ice film at ~3390 cm^{-1} (O–H stretch) and ~1630 cm^{-1} (scissors). In addition, relatively sharp peaks of AN appear with lower intensities at 3002 cm^{-1} (asymmetric CH stretch), 2941 cm^{-1} (symmetric CH stretch), 2415 cm^{-1} (symmetric CH bend + CH_3 rock), 2289 cm^{-1} (symmetric CH bend + CC stretch), 2252 cm^{-1} (CN stretch), 1455 cm^{-1} (asymmetric CH bend), 1422 cm^{-1} (CH_3 rock + CN bend), 1378 cm^{-1} (symmetric CH bend), and 1038 cm^{-1} (CH_3 rock).[34] Among these, C≡N stretch mode (2252 cm^{-1}) uniquely exhibits the strong Stark effect.

Figure 4(b) displays the absorption spectrum $[A(\bar{\nu})]$ of υ(C≡N) on a magnified scale. Its Stark difference spectrum, $[\Delta A(\bar{\nu})]$, which is the absorption in the presence of applied electric field minus the absorption without the field, is shown in Fig. 4(c). In this figure, the absorption intensities at peak sides (near 2255 cm^{-1} and 2248 cm^{-1}) gradually increase with longer exposure of Cs^+, while the intensity of the peak center (2252 cm^{-1}) decreases. These changes clearly show that υ(C≡N) peak is broadened by the applied field. Here, VSE appeared as peak broadening rather than as a shift in one direction, because the molecular orientations of AN in the sample were isotropic. The poling of AN molecules by the applied field did not seem to occur. We did not observe any further change in the υ(C≡N) spectral shape related to the poling when the sample was left in a charged state for a long time or when its temperature was raised to ∼120 K.

The Stark effect on the υ(C≡N) stretch mode was analyzed following the method of Andrews and Boxer,[5,7] which was developed for nitrile compounds with isotropic molecular orientation in glassy samples. The theoretical background and physical model for the Stark analysis have been detailed previously.[5,7] Briefly, VSE yields a slight peak shift for each molecule under electric field, which is expressed as Eq. (2) in an approximate form:

$$\Delta\bar{\nu} = -\frac{1}{hc}\left(\boldsymbol{\Delta\mu}\cdot\mathbf{F} + \frac{1}{2}\mathbf{F}\cdot\boldsymbol{\Delta\alpha}\cdot\mathbf{F}\right), \tag{2}$$

where $\boldsymbol{\Delta\mu}$ is the dipole moment difference between the ground and excited states, often called the difference dipole moment or Stark tuning rate, $\mathbf{F}$ is the local electric field, and $\boldsymbol{\Delta\alpha}$ is the difference polarizability. Integrating the peak shifts over all orientations of molecules, combined with the shape of the absorption spectrum $[A(\bar{\nu})]$ and the changes in transition dipole moment ($\mathbf{M}$), yields a computed Stark difference spectrum. Following the derivation in Ref. 5, the Stark difference spectrum can be expressed as the sum of frequency-weighted derivatives of the absorption spectrum, written as Eq. (3):

$$\Delta A(\bar{\nu}) = \alpha A(\bar{\nu}) + \beta\bar{\nu}\frac{\partial}{\partial\bar{\nu}}\frac{A(\bar{\nu})}{\bar{\nu}} + \gamma\bar{\nu}\frac{\partial^2}{\partial\bar{\nu}^2}\frac{A(\bar{\nu})}{\bar{\nu}}. \tag{3}$$

The third and higher order terms in the derivative expansion are neglected in this expression. Here, α, β, and γ are empirical coefficients for the zeroth, first, and second derivative terms, respectively; they are proportional to $|\mathbf{F}|^2$ and are specific functions of the Stark parameters of the molecule, including $\boldsymbol{\Delta\mu}$, $\boldsymbol{\Delta\alpha}$, and $\mathbf{M}$. These functional forms are given in Ref. 5. We obtained α, β, and γ by fitting this mathematical equation to the experimental Stark difference spectrum. If the Stark parameters of the molecule are known, the field strength can be deduced from the α, β, and γ values. Alternatively, if the field strength is known, the Stark parameters can be deduced experimentally. In the case of isotropically distributed molecules, γ is the most important empirical coefficient of Eq. (3) for making the fit. In practice, in first-order approximation, the optimization of only γ was sufficient to estimate the electric field strength from known $|\boldsymbol{\Delta\mu}|$.

Figure 5 shows the electric fields deduced from the VSE analysis of Stark difference spectra presented in Fig. 4(c). The results of Kelvin probe measurements recorded simultaneously with VSE measurements are also shown for comparison. The Kelvin probe measurements estimate the external electric field, $\mathbf{E}$, by dividing the measured film voltage with the film thickness. The dielectric polarization of the medium induced by the field is taken into account in terms of ε_r in Eq. (1). By comparison, the VSE method monitors the local field at the position of the probe molecule, as mentioned above. The local field is related to the external field by $\mathbf{F} = f\mathbf{E}$. For calculating the electric field strength in the VSE analysis, we used $|\boldsymbol{\Delta\mu}|/f = 0.0258$ D, which is the Stark parameter for AN determined by Andrews and Boxer[5,7] from their VSE measurements at the field strength of 9×10^7 V m^{-1}. We assume that the value of f is unity for comparing the field strengths estimated from VSE and Kelvin probe in Fig. 5. The figure shows that VSE gives a lower field strength than Kelvin probe for long ion-exposure times (10–20 min) or at high applied fields. The two measurements agree with each other (1.5×10^8 V m^{-1} vs. 1.7×10^8 V m^{-1}) at the ion-exposure time of 5 min, whereas VSE gives slightly higher field than Kelvin probe at shorter exposure time (2 min). The discrepancy between the two results is discussed in Sec. IV.

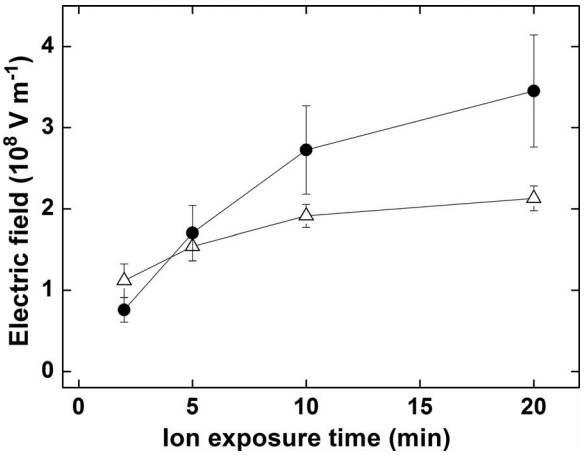

FIG. 5. Estimated electric fields from the results of Kelvin probe (●) and VSE (△) measurements. The sample was the same as the one used for Fig. 4, with the structure of H_2O(21.3 nm)/AN(17.9 nm)/H_2O(27.4 nm)/Ru(0001). The VSE data are from the Stark difference spectra shown in Fig. 4(c), and the field was estimated using $|\boldsymbol{\Delta\mu}|/f = 0.0258$ D with $f = 1.0$. The error bar for VSE is estimated from the spectral noise level.

IV. DISCUSSION

Figure 5 shows that VSE and Kelvin probe measurements produce mutually agreeing fields at moderate field strengths ($(1–2) \times 10^8$ V m^{-1}), but a significant difference at higher field strengths. Because the Kelvin probe method gives accurate measurement of the film voltage over a wide range of voltages, the uncertainty in the estimated field in this method is mostly due to uncertain sample parameters. The sample parameters are not field-dependent variables, i.e., if an error is introduced by these parameters, it will appear consistently without changing with the field strength. The VSE and Kelvin probe results meet each other in the field region of $(1–2) \times 10^8$ V m^{-1}, which is close to the field (9×10^7 V m^{-1}) at which the $|\boldsymbol{\Delta\mu}|$ value used in this work was determined in

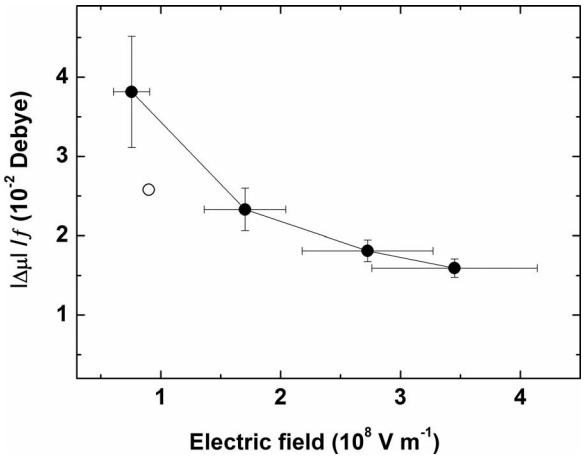

FIG. 6. Difference dipole moment ($|\boldsymbol{\Delta\mu}|/f$) of AN used for the VSE analysis of υ(C≡N) peak at various field strengths. Kelvin probe results were used as a field reference for calculating $|\boldsymbol{\Delta\mu}|/f$ (see text). Open circle is the $|\boldsymbol{\Delta\mu}|/f$ value reported in Ref. 5.

previous VSE works.[5,7] Therefore, this overlapping is a good indicator that we have correctly converted the film voltage data into the internal field strength. If the conversion procedure is correct, Kelvin probe can be regarded as a more reliable method than the VSE method, because the former gives consistent field measurements over a wider range.

The field strength estimation from the VSE measurement requires the analysis of Stark difference spectra using a model function that contains mathematical approximation. For example, the model function is expanded into a series form with respect to the frequency shift ($\Delta\upsilon$), and its higher order terms are neglected in Eq. (3). Consequently, the accuracy of the analysis is reduced when $\Delta\upsilon$ (or field strength) is high. We believe that this approximation is an important cause of the discrepancy between the VSE and Kelvin probe results appearing at high fields. Note that the present device produces higher fields than those in previous studies.[5,7] Other possible causes of the discrepancy may include the fact that Andrews and Boxer[5,7] used dilute samples of AN embedded in a solvent, whereas the present work used a dense AN layer trapped between ice films. As long as the local field correction is concerned, both samples are prepared in frozen molecular solid forms and thus their f values may not be drastically different.[33] For closer comparison of the results of two studies, we prepared dilute AN samples by codepositing AN and water in 1:5 ratio at 70–120 K. RAIRS experiments with these samples showed a υ(C≡N) peak with a full width at half maximum of about 20 cm^{-1}, much broader than that of an AN-sandwich film, indicating that dispersed AN molecules had microscopically heterogeneous solvation structures in amorphous solid water. The υ(C≡N) peak shape changed with sensitive correspondence to annealing temperature, probably due to changes in the AN solvation structure. These features hampered accurate VSE measurements for the dilute AN samples.

To match the VSE and Kelvin probe results over the entire investigated field range, we need to consider $|\boldsymbol{\Delta\mu}|$ as a field-dependent variable. We stress that this assumption is made only to fit the VSE data over a wide field range, using a simple spectral shape function that is appropriate only in a narrow range in low fields. Though not a rigorous approach, it could make the VSE analysis easier once the field-dependence of $|\boldsymbol{\Delta\mu}|$ is numerically determined by other means. Among all Stark parameters, $|\boldsymbol{\Delta\mu}|$ is the most important coefficient in the linear Stark effect. To deduce the value of $|\boldsymbol{\Delta\mu}|$ at various field strengths, we use the field curve from the Kelvin probe measurement as a reference and fit the VSE curve to it. The result is shown in Fig. 6. The figure shows that $|\boldsymbol{\Delta\mu}|$ decreases by approximately 60% as the field increases from 7.6×10^7 V m^{-1} to 3.5×10^8 V m^{-1}. Also marked in the figure is $|\boldsymbol{\Delta\mu}|$ measured by Andrews and Boxer,[5] which is in reasonable agreement with our $|\boldsymbol{\Delta\mu}|$ curve within experimental uncertainties.

V. SUMMARY

This work demonstrates that strong electric field can be generated inside an ice film by depositing Cs^+ ion beams onto the film. Unlike conventional devices that use electrically biased metal plates, the present device is charged by using thermodynamic energy that traps Cs^+ ions on the ice film surface. The internal field of the charged film was estimated through the measurements of film voltage using a Kelvin probe and the vibrational Stark shift of AN trapped in the sample. The two methods gave agreeable results in the field region (1–2) $\times 10^8$ V m^{-1}, where the current VSE analysis model is mostly applicable. It was shown that the field strength can be increased to 4.2×10^8 V m^{-1} (or 2.1×10^8 V m^{-1}) inside the AN (or H_2O) layer after the Cs^+ beam exposure to saturation, which is approximately one order higher than the field strength achievable by conventional capacitor methods.

Besides the generation of unprecedentedly strong electrostatic fields in an ice film, the present method has potential advantages in investigating the effects of electric field on condensed-phase molecular systems. For example, controlling the composition and structure of the sample in molecular scale is easy by means of thin-film-growing methods developed in UHV. Also, surface spectroscopic techniques can be used for monitoring physicochemical changes that the sample undergoes under the field, as illustrated in the present work for the measurements with RAIRS and work function probe. With such characteristics, we anticipate that the ice film capacitor will find wide applications in studying molecular systems under strong electric fields in condensed phase. Research efforts currently underway in our laboratory include the study of charged ice films as a UHV model of EDLs.

ACKNOWLEDGMENTS

This work was supported by the grant of the National Research Foundation (NRF) of Korea funded by the Korea government (MSIP) (Grant No. 2007-0056095).

[1]R. Parsons, Chem. Rev. **90**(5), 813–826 (1990).
[2]M. J. Weaver and X. P. Gao, Annu. Rev. Phys. Chem. **44**, 459–494 (1993).
[3]P. C. Hiemenz and R. Rajagopalan, *Principles of Colloid and Surface Chemistry*, 3rd ed. (Taylor & Francis, 1997).
[4]H. Labhart, Adv. Chem. Phys. **13**, 179–204 (1967).
[5]S. S. Andrews and S. G. Boxer, J. Phys. Chem. A **104**(51), 11853–11863 (2000).

[6]E. S. Park, M. R. Thomas, and S. G. Boxer, J. Am. Chem. Soc. **122**(49), 12297–12303 (2000).
[7]S. S. Andrews and S. G. Boxer, J. Phys. Chem. A **106**(3), 469–477 (2002).
[8]D. K. Lambert, J. Chem. Phys. **89**(6), 3847–3860 (1988).
[9]Y. H. Yoon, D. H. Woo, T. Shin, T. D. Chung, and H. Kang, J. Phys. Chem. C **115**(35), 17384–17391 (2011).
[10]E. M. Stuve, Chem. Phys. Lett. **519–520**, 1–17 (2012).
[11]H. Stapelfeldt and T. Seideman, Rev. Mod. Phys. **75**(2), 543–557 (2003).
[12]J. Cyriac, T. Pradeep, H. Kang, R. Souda, and R. G. Cooks, Chem. Rev. **112**(10), 5356–5411 (2012).
[13]A. A. Tsekouras, M. J. Iedema, and J. P. Cowin, Phys. Rev. Lett. **80**(26), 5798–5801 (1998).
[14]K. Wu, M. J. Iedema, and J. P. Cowin, Science **286**(5449), 2482–2485 (1999).
[15]R. C. Bell, K. Wu, M. J. Iedema, G. K. Schenter, and J. P. Cowin, J. Am. Chem. Soc. **131**(3), 1037–1042 (2009).
[16]S. A. Miller, H. Luo, S. J. Pachuta, and R. G. Cooks, Science **275**(5305), 1447–1450 (1997).
[17]Y. Horowitz and M. Asscher, J. Chem. Phys. **136**(13), 134701 (2012).
[18]M. Michaud, A. Wen, and L. Sanche, Radiat. Res. **159**(1), 3–22 (2003).
[19]R. Balog, P. Cicman, D. Field, L. Feketeova, K. Hoydalsvik, N. C. Jones, T. A. Field, and J. P. Ziesel, J. Phys. Chem. A **115**(25), 6820–6824 (2011).
[20]S. C. Park, E. S. Moon, and H. Kang, Phys. Chem. Chem. Phys. **12**(38), 12000–12011 (2010).
[21]J. H. Kim, Y. K. Kim, and H. Kang, J. Phys. Chem. C **111**(22), 8030–8036 (2007).
[22]E. S. Moon, Y. Kim, S. Shin, and H. Kang, Phys. Rev. Lett. **108**(21), 226103 (2012).
[23]H. Kang, Bull. Korean Chem. Soc. **32**(2), 389–398 (2011).
[24]A. Hodgson and S. Haq, Surf. Sci. Rep. **64**(9), 381–451 (2009).
[25]D. N. Denzler, S. Wagner, M. Wolf, and G. Ertl, Surf. Sci. **532–535**, 113–119 (2003).
[26]S. Haq and A. Hodgson, J. Phys. Chem. C **111**(16), 5946–5953 (2007).
[27]T. Kondo, H. S. Kato, M. Bonn, and M. Kawai, J. Chem. Phys. **126**(18), 181103 (2007).
[28]H. Kang, Acc. Chem. Res. **38**(12), 893–900 (2005).
[29]D. E. Brown, S. M. George, C. Huang, E. K. L. Wong, K. B. Rider, R. S. Smith, and B. D. Kay, J. Phys. Chem. **100**(12), 4988–4995 (1996).
[30]B. Torrie and B. Powell, Mol. Phys. **75**(3), 613–622 (1992).
[31]J. Barthel, K. Bachhuber, R. Buchner, J. B. Gill, and M. Kleebauer, Chem. Phys. Lett. **167**(1–2), 62–66 (1990).
[32]J. Barthel, K. Bachhuber, R. Buchner, and H. Hetzenauer, Chem. Phys. Lett. **165**(4), 369–373 (1990).
[33]G. U. Bublitz and S. G. Boxer, Annu. Rev. Phys. Chem. **48**(1), 213–242 (1997).
[34]J. E. Schaff and J. T. Roberts, Langmuir **15**(21), 7232–7237 (1999).